(Received 9 October 2023, Accepted 6 December 2023, Scheduled 15 December 2023)

Innovative Loaded Low-Profile Tri-Band MIMO Antenna System for Wi-Fi 7 Technology

Ahmad Yacoub* and Daniel N. Aloi

Electrical and Computer Engineering Department, Oakland University, Rochester Hills, MI, USA

ABSTRACT: A distinctive low-profile 2 × 2 MIMO antenna system for Wi-Fi 7 applications is presented in this paper that is compact, easily manufactured and with excellent performance. Because of its compact size and good RF performance, the design can be placed in hidden locations for various applications such as the automotive field in the front side mirrors or front dashboard, and consumer products in laptops and internet wireless routers. The proposed design can cover the entire tri-bands of Wi-Fi 7 (2400–2495 MHz, 5150–5895 MHz, 5945–7125 MHz) using a loaded low-profile Planar Inverted-F Antenna (PIFA) with distinct dimensions and slots across its geometry. The element design and the MIMO system is simulated and a properly made prototype was fabricated to present the results in terms of reflection coefficients, current distribution, combined radiation patterns, passive isolation, ports efficiencies, and Envelope Correlation Coefficient (ECC). The design shows relatively good RF properties across the entire three bands, hence making it an attractive solution to be used for Wi-Fi 7 technology to satisfy the needs of larger omnidirectional coverage area, wider channel bandwidth, and better transmission rates with low interference.

1. INTRODUCTION

Wireless technologies have advanced dramatically in the last 20 years in practically every consumer product, from personal computers and wearable technology to smart cars. Wireless Local Area Network (WLAN) and cellular 5G are two important communication technologies that have undergone rapid development in multiple fields in order to provide high throughput rates, low latency, increased network capacity, and cost-effective solutions for all consumers [1–3]. WLAN is becoming a crucial part in Internet-of-Things (IoT) where smart nodes are connected for better automated society and living quality [4]. WLAN uses the IEEE 802.11 wireless standard, and the most recent version, 802.11 ax, was adopted in 2019 which supports Wi-Fi 6, Wi-Fi 6E. Wi-Fi 6 covers two bands: 2.4 GHz band (2400–2495 MHz), which offers the most coverage but at a lower data rate, and 5 GHz band (5150–5925 MHz), which has a significantly better throughput but a smaller coverage area due to wave propagation losses.

Wi-Fi 6E extends the frequency bands to 6 GHz (5945–7125 MHz) which offers smaller coverage area than 2G/5G bands but supports a maximum throughput of 1.2 Gbps for high order modulation of 1024 Quadrature Amplitude Modulation (QAM) and wide channel bandwidth of 160 MHz [5, 6].

The forthcoming IEEE 802.11 standard, also referred to as Wi-Fi 7, has its main goal of enhancing speed rate to 40 Gbps. In comparison to previous Wi-Fi technology, which only allowed devices to connect to one channel band (2.4 GHz, 5 GHz, or 6 GHz), it introduces double channel bandwidth for a maximum of 320 MHz and four times higher modulation rates for a maximum of 4096 QAM. Wi-Fi 7 also presents Multi Link Operation (MLO) algorithm, which enables devices to transmit and receive data simultaneously over multiple frequency bands and channels [7, 8].

Multiple-Input Multiple-Output (MIMO) antenna systems must be created in order to meet the enhanced needs for wider channel bandwidth and higher modulation order for Wi-Fi 7 technology. MIMO systems increase the overall throughput without increasing the operating frequency channels or transmit power since it uses multiple antennas on both the transmitter and receiver which also provides diversity that reduces multipath effect [9]. It is also essential for Wi-Fi 7 applications to have MIMO antenna systems with better passive isolation between antennas (low envelope correlation coefficient). Higher isolation provides enhanced Error Vector Magnitude (EVM) for higher order modulation (4K QAM) and improved Rate vs Range (RvR) coverage area [10, 23].

The performance of the MIMO antenna system is typically affected by several factors. Physical constraints, size restrictions, and mutual coupling between various antennas provide difficult problems, particularly if the antennas are housed together in a single housing. These factors make it difficult to achieve MIMO performance standards for ports efficiencies, passive isolation, and ECC, particularly when several applications, such as Wi-Fi, Bluetooth, cellular 5G, and Global Navigation Satellite System (GNSS), are implemented in a single housing [11].

In this paper, a distinctive low-profile loaded PIFA with unique slots has been developed for Wi-Fi 7 hidden-location applications such as front side mirrors or front dashboard in automotive and consumer products in laptops and internet access points. The design has a unique shape and physical dimensions which makes it suitable for these applications. The proposed design can cover wide tri-band frequencies (2.4 GHz–

* Corresponding author: Ahmad Yacoub (ahmadyacoub@oakland.edu).

2.5 GHz/5.15 GHz–7.125 GHz) with reasonably small dimensions because of its unique shape, using unique slots in the horizontal plane, and being loaded on low-cost Flame Retardant (FR4) material without major losses in antenna performance. Additionally, a 2×2 MIMO antenna system is examined to meet the high-performance demands of Wi-Fi 7 standards. The proposed MIMO system was able to achieve good performance and isolation between elements by optimizing the spatial distance and orientation of each antenna as well as changing the shape of the ground plane, which enhances passive isolation without increasing the spatial distance between the elements, especially at lower frequency bands. Compared to existing work in literature [12], the authors present Wi-Fi 6E antenna for laptops that works in 2.4 GHz, 5 GHz, and 6 GHz bands; however, the height of the element is relatively high, and the efficiency at the low band is less than 40%. In [13–15], the antenna elements work in the Wi-Fi 6E tri-bands, but the size of each element is relatively bigger than the proposed design in this work, and the efficiency and peak gain in the 2.4 GHz band is less than 40% and 2 dBi, respectively. The antenna MIMO systems presented in [16–18] present a good performance for Wi-Fi 6E applications in terms of return loss, passive isolation, and radiation pattern; however, passive isolation across MIMO elements needs to be improved in order to meet the high modulation rate (4K QAM) requirements for Wi-Fi 7. A comparison summary between the research given in this paper and the previous literature is summarized in Table 3.

High Frequency Structure Simulator (HFSS) simulation software was used to model the antenna design and MIMO system, and then a proper element prototype was built and measured on a 100 mm ground plane inside an anechoic chamber to present practical measurements for the proposed design. The results are presented in terms of return loss, passive isolation, radiation pattern, surface current distribution, antenna ports radiation efficiencies, Envelope Correlation Coefficient (ECC), and Diversity Gain (DG).

The following sections make up this paper. Section 2 describes the proposed antenna design, geometrical characteristics, simulation and measurement setups, and RF performance of the specific element. The proposed MIMO antenna system, as well as its MIMO features and performance, is presented in Section 3 along with a table of comparison to prior work in the literature.

2. PROPOSED ANTENNA DESIGN AND MEASUREMENTS

The design consists of a loaded Planar Inverted F-antenna (PIFA) antenna on FR4 material with dielectric constant (ϵ_r) of 4.4, permeability of 1, and loss tangent of 0.025. It is a good choice as a substrate material because of its high mechanical strength, insulating properties, and affordability. Fig. 1 and Table 1 show the antenna layout and its optimized geometrical parameters with the total dimensions of 3 mm (height) $\times$ 14.5 mm (length) $\times$ 17 mm (width).

The PIFA is the basis for the suggested design in this work. However, distinct physical dimensions and slots are added in the horizontal plane, resulting in a lower low band operating frequency, a wider bandwidth, and a smaller occupied volume than those described in existing literature. The design is made of a metal sheet with dimensions of 3 mm (H) $\times$ 14.5 mm (L) $\times$ 17 mm (W), and it is loaded with FR4 material with thickness of 0.3 mm as shown in Fig. 1 with top and side views of the simulated model. The location of the feeding plate is optimized at the middle-right side of the horizontal plane which is important for the 5 GHz/6 GHz bands to create a wideband folded monopole structure with a U-shaped slot. The shorting plate is placed at the edge of the horizontal plane with a tuned width W_s and specific distances from the feeding plate L_b and horizontal edge W_d to control the resonance frequency of the low band (2.4 GHz). The proposed design introduces two new ladder-shape structures containing rectangular slots with width I_w and length I_L which lowers the resonance frequency at 2.4 GHz band without increasing the antenna size and acts as RF choke for high frequency bands which improves return loss and radiation properties at 5 GHz/6 GHz.

As a general design guideline, the low frequency band (2.4 GHz) is determined by the physical volume of the antenna in addition to feeding and shorting plates dimensions. Equation (1) provides an analytical method to accurately approximate the resonance frequency of the low band of the conventional PIFA antenna [19]:

$$f_c = \frac{c}{3W + 5.6L + 3.7H - 3W_f - 3.7W_s - 4.3W_d - 2.5L_b} \quad (1)$$

TABLE 1. Optimized geometrical parameters of the proposed design.

Parameter	Value (mm)
W	17
L	14.5
H	3
S_w	11
S_L	10.2
W_S	10
W_f	2.15
W_d	4.26
L_b	10.17
S_p	1.1
I_W	1.51
I_L	0.74

Calculating f_c using Equation (1) yields center frequency of 3.4 GHz; however, using U-shape and ladder-shape slots creates a longer path for radiating current which supports longer wavelengths, hence lowering the frequency response. In addition, loading the element with FR4 material reduces the antenna dimensions to result in the final tuning to the center frequency of (2.45 GHz). For 5 GHz and 6 GHz bands, the structure of the feeding plate up until U-shape slot acts as a folded monopole structure ($\lambda/4$) loaded on an FR4 substrate to get the resonance frequency around 6 GHz. The width of the U-shape slot S_w and the length S_L control the volume occupied by the monopole structure, hence optimizing the operating bandwidth to cover both 5 GHz and 6 GHz bands. The ladder-shape

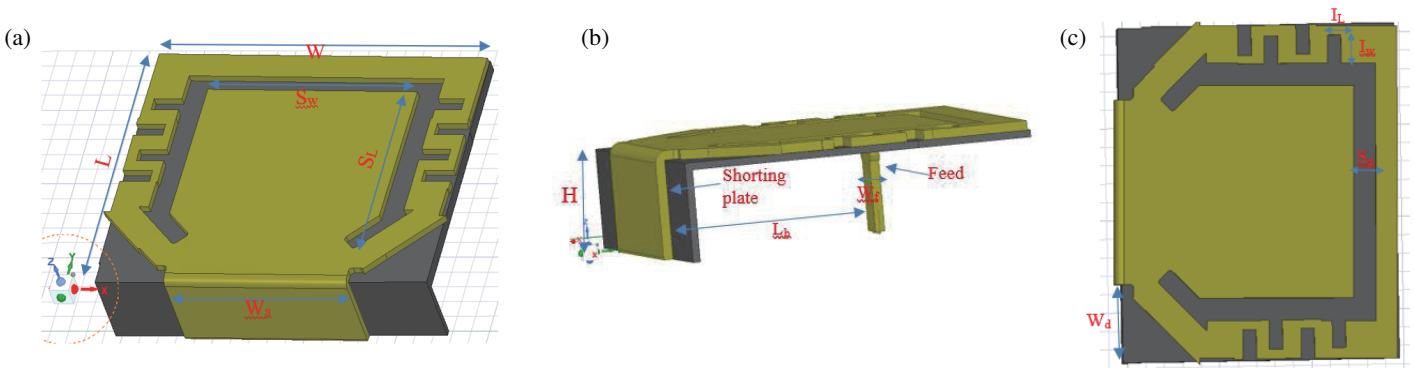

FIGURE 1. Proposed Wi-Fi 7 antenna: (a) top and side view, (b) right side view, and (c) top side view.

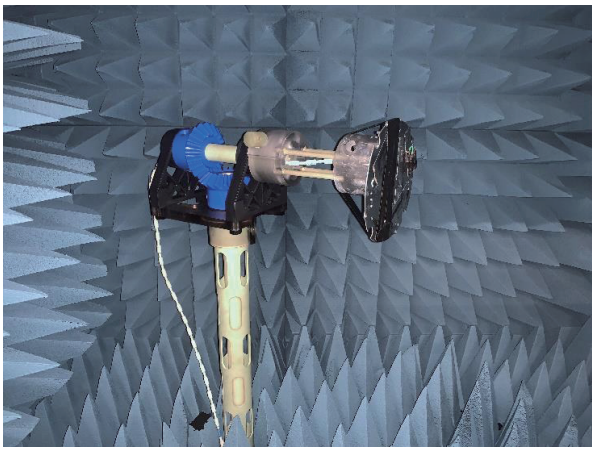

FIGURE 2. Antenna setup inside the anechoic chamber.

structures also act as high impedance inductors for high frequency bands which prevents the current from leaking to the horizontal plate, hence improving radiation performance at the 5 GHz/6 GHz bands.

Table 2 presents the antenna design goals and performance requirements for Wi-Fi 7 technology to meet high-speed rates and adequate coverage area. Table 2 shows the antenna performance in terms of polarization, return loss, passive isolation, port efficiencies, peak gain, and ECC.

TABLE 2. Antenna's design goals and performance requirements.

Parameter	Value
Polarization	Linear
Return loss	10 dB
Passive isolation	30 dB
Port efficiencies	$> 70\%$
Peak gain	2–3 dBi
ECC	< 0.1

The design is simulated using full wave solver in Ansys HFSS software that uses Finite Element Method (FEM) to analyze antenna structures. Then, a properly-built prototype is measured on a small ground plane (120 mm in diameter) inside an anechoic chamber. The setup of the antenna inside the chamber is shown in Fig. 2 where a U.FL to SMA connector is used between the antenna feed and the coaxial cable of the chamber.

The proposed design's simulated and measured reflection coefficients are contrasted in Fig. 3. The results show that the return loss performance in all Wi-Fi 7 bands is better than 8 dB. With slight variations caused by antenna positioning on the ground plane and minor cable loss across frequency bands, Fig. 3 also demonstrates reasonable agreement of antenna impedance between simulated design and fabricated prototype. Fig. 4 shows the effect on impedance matching of the ladder-shape slots that are placed on the horizontal plane of the element. The low band (2.4 GHz) gets tuned lower without increasing the physical dimensions, and the return loss gets improved by 1–2 dB in the high bands (5 GHz/6 GHz) since the ladder-shape slots act as an RF choke and prevent the current from leaking into the horizontal plane. The 5 GHz and 6 GHz structure (folded monopole) has a center frequency resonance at around 5.8 GHz. The width and volume occupied by this structure control the covered bandwidth from 5.15 GHz to 7.125 GHz. However, the RF cable with U.FL connector generates some ripples in the impedance measurements, especially at high frequencies due to cable length, bends, and connector's stability.

Figure 5 presents the magnitude of the surface current distribution measured in dB. It can be concluded that in the 2.4 GHz

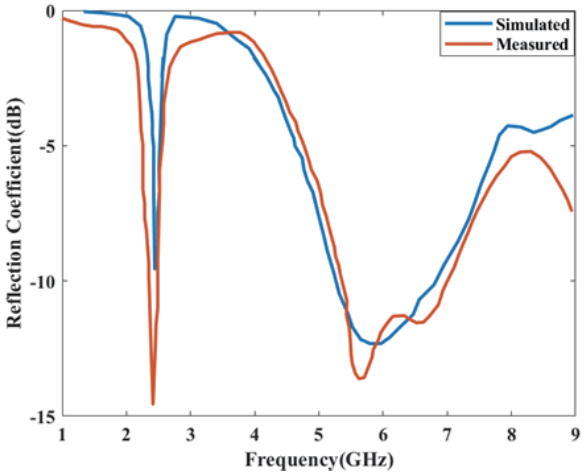

FIGURE 3. Reflection coefficient in dB for simulated and fabricated element.

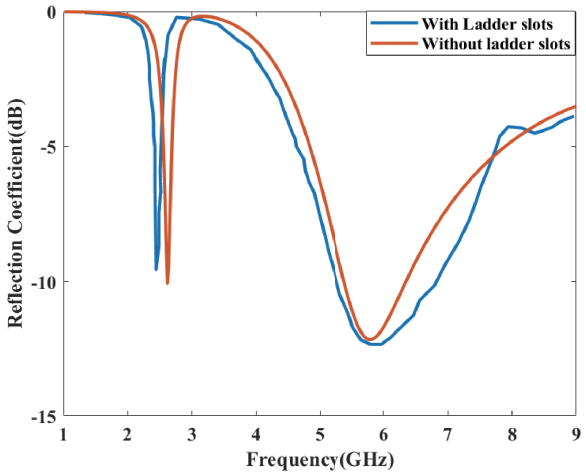

FIGURE 4. Comparison of reflection coefficient in dB for simulated model with and without ladder slots.

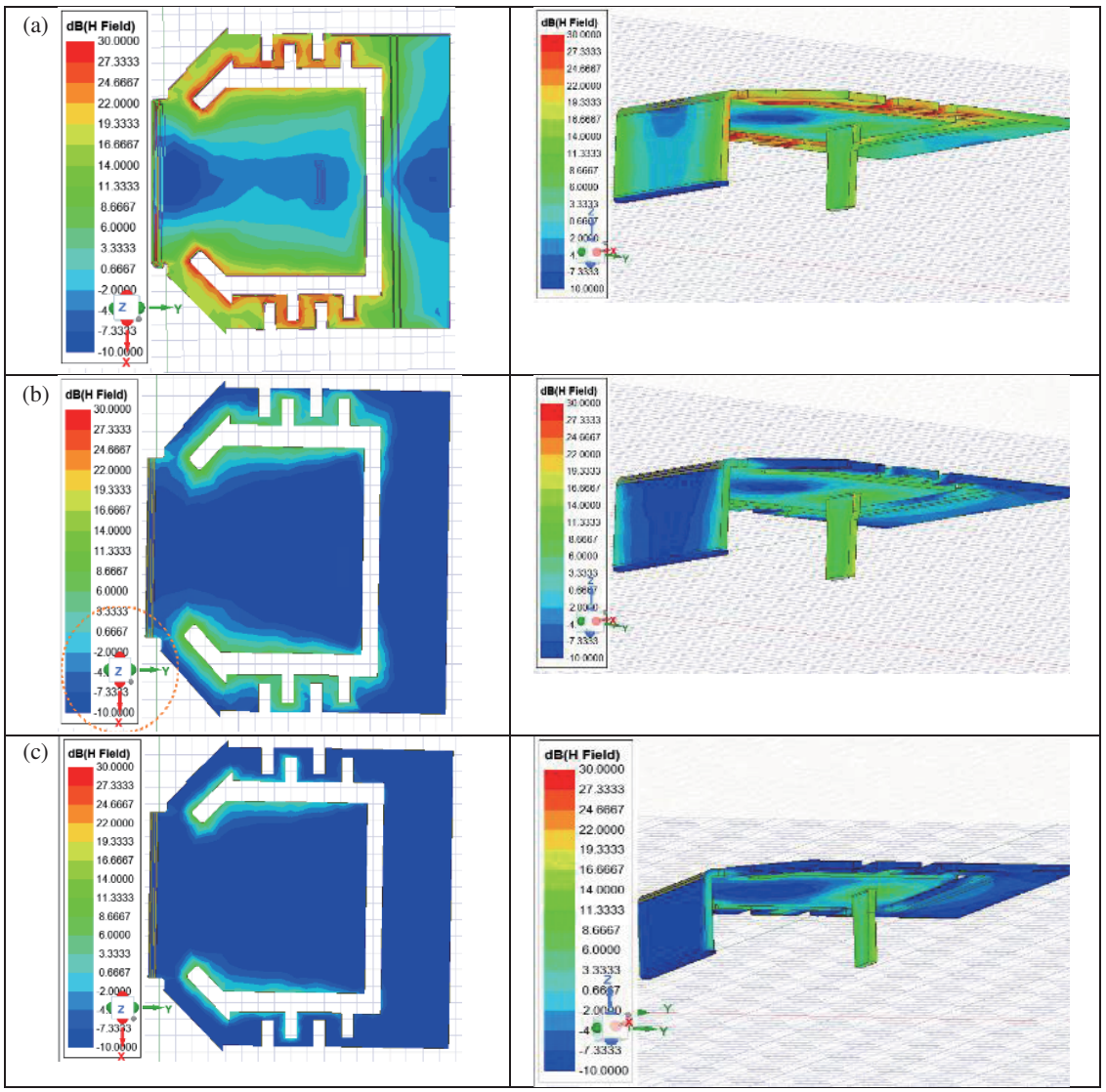

FIGURE 5. Magnitude of surface current distribution measured in dB on the top and right side of the antenna for: (a) 2.45 GHz, (b) 5.5 GHz, and (c) 6.5 GHz.

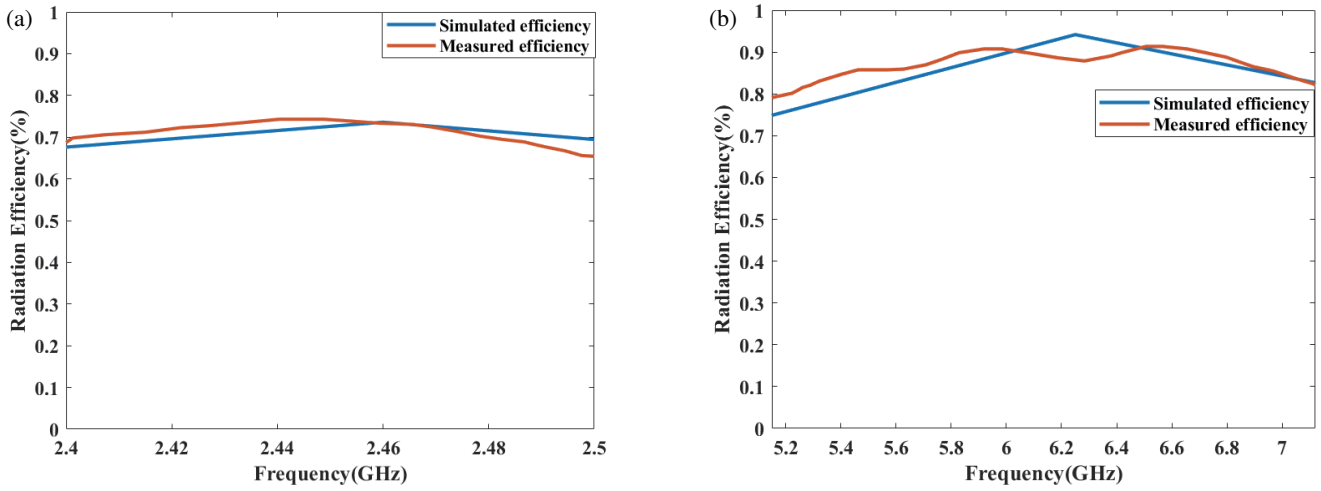

FIGURE 6. Antenna radiation efficiency for simulated and fabricated model: (a) 2,4 GHz band, and (b) 5 GHz and 6 GHz bands.

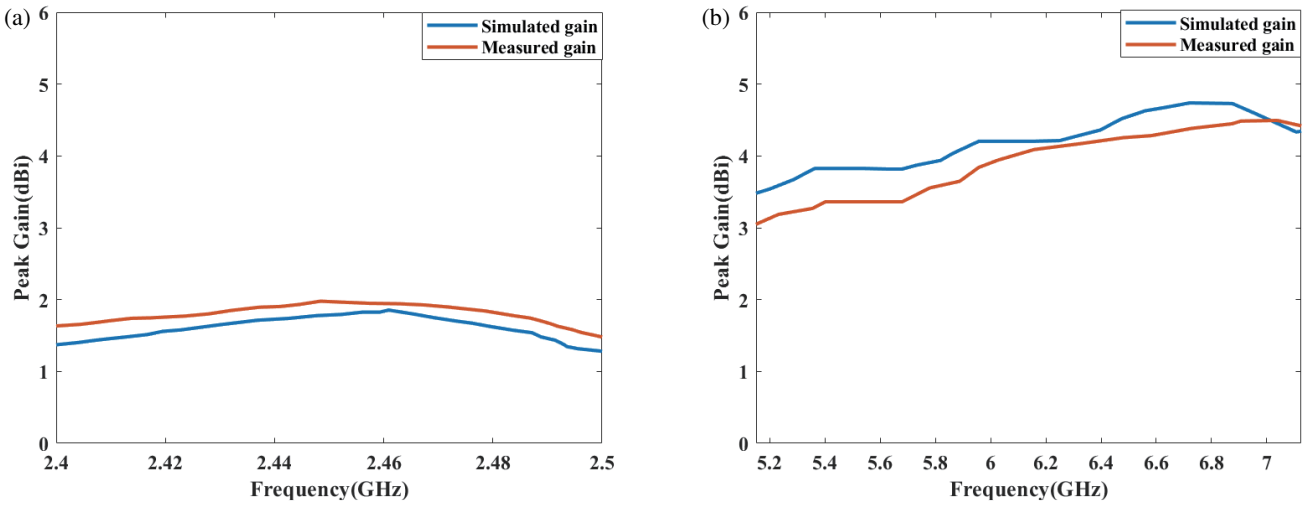

FIGURE 7. Antenna's peak gain measured in dBi: (a) 2,4 GHz band, and (b) 5 GHz and 6 GHz bands.

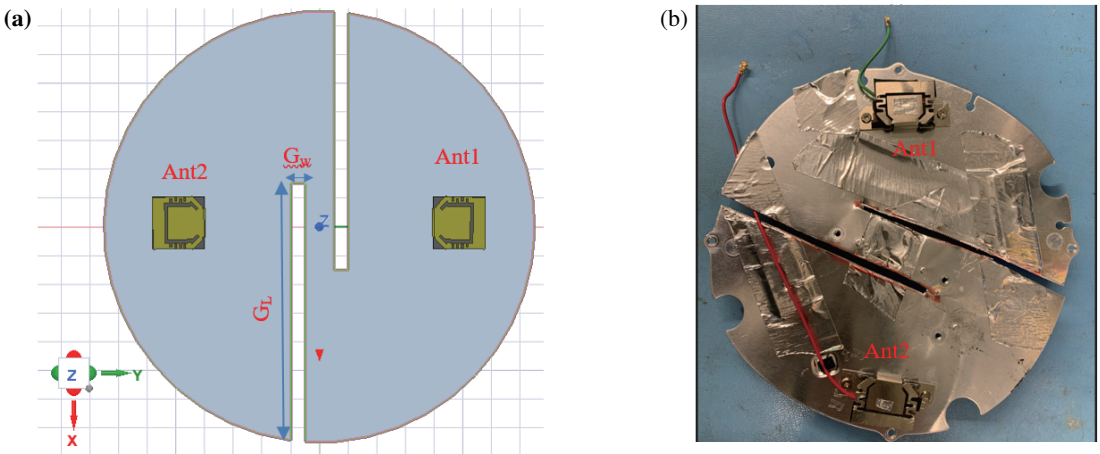

FIGURE 8. Simulation model and fabricated prototype for the proposed MIMO system: (a) simulation model, and (b) fabricated prototype.

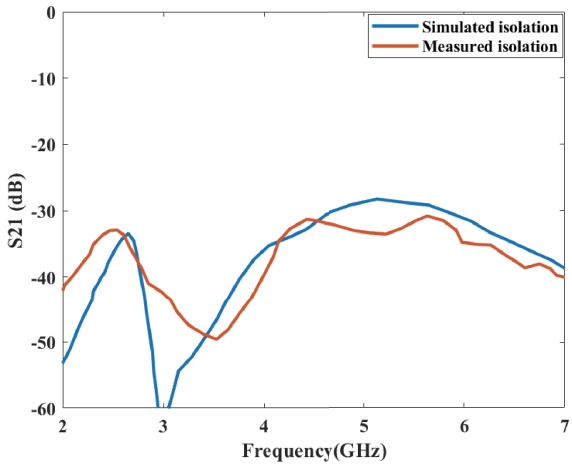

FIGURE 9. Simulated and measured passive isolation in dB for the Wi-Fi 7 MIMO system.

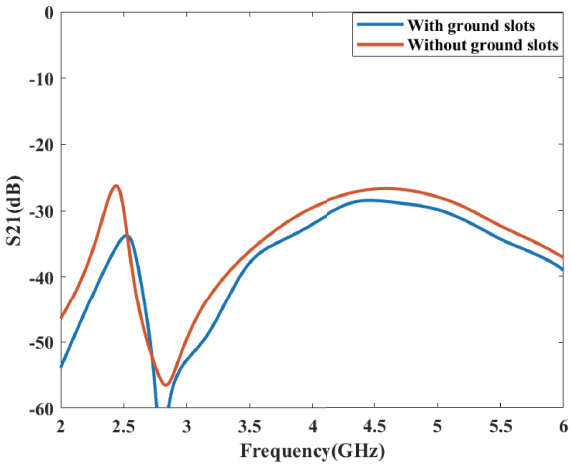

FIGURE 10. Comparison of passive isolation with and without ground plane slots.

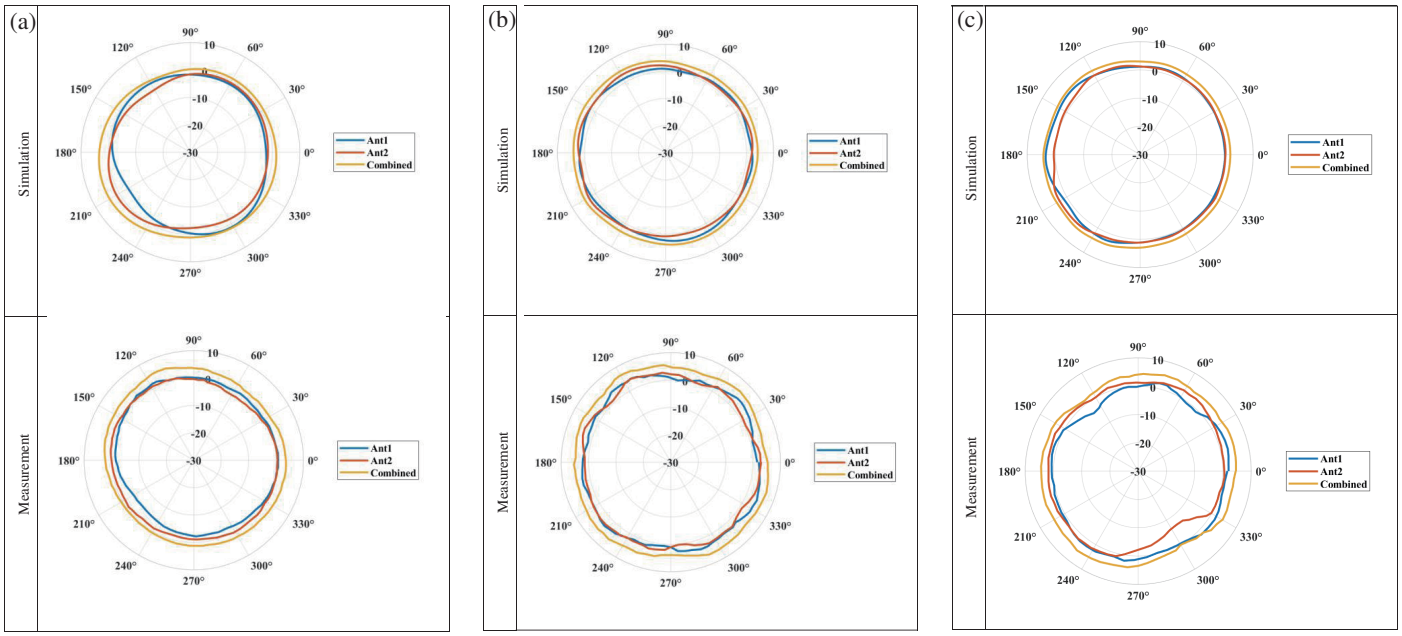

FIGURE 11. Horizontal cuts of radiation pattern measured in dBi at theta = 60 degrees for the simulated and fabricated model of the Wi-Fi 7 MIMO system: (a) 2.45 GHz, (b) 5.5 GHz, and (c) 6.5 GHz.

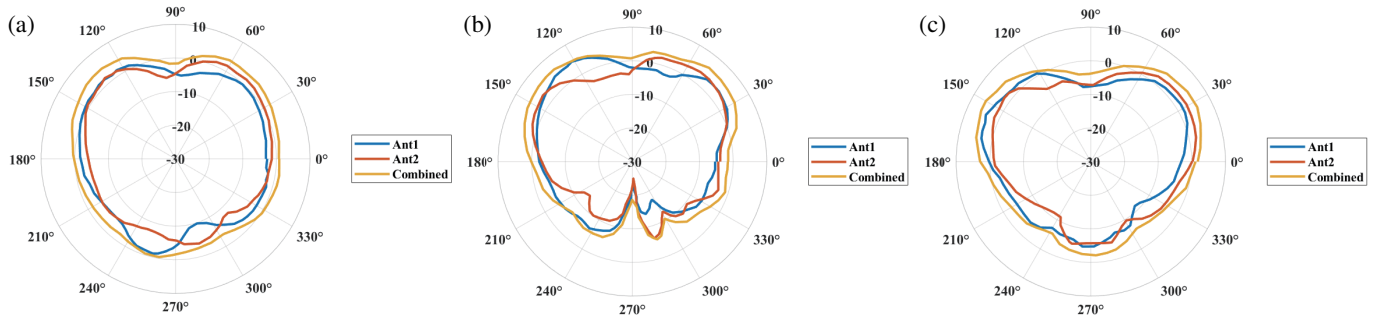

FIGURE 12. Vertical cuts of radiation pattern measured in dBi across elevation at phi = 0 degrees for the simulated and fabricated model of the Wi-Fi 7 MIMO system: (a) 2.45 GHz, (b) 5.5 GHz, and (c) 6.5 GHz.

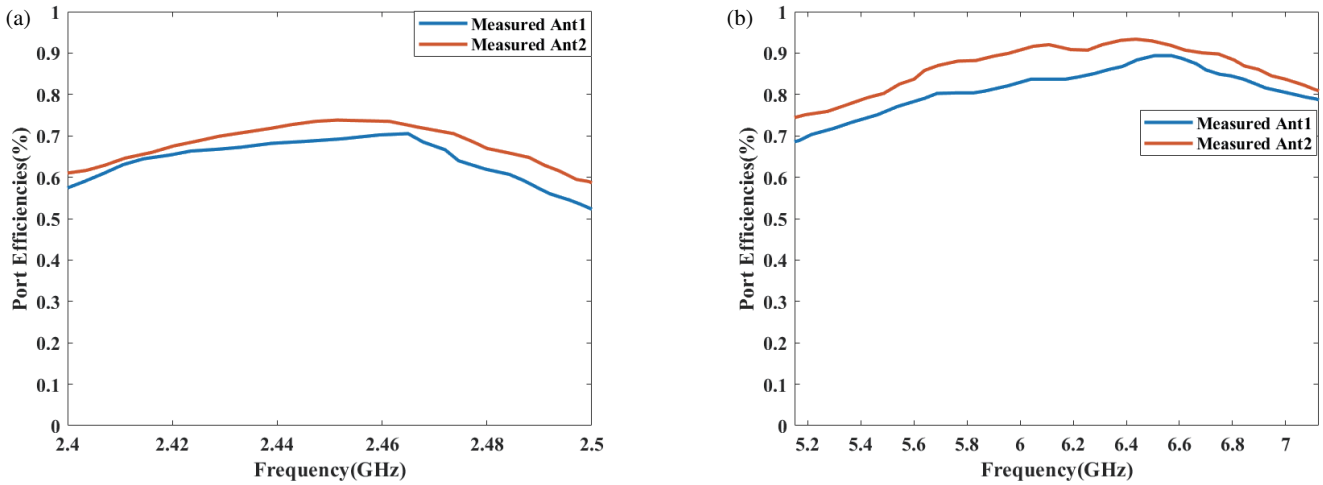

FIGURE 13. Measured port radiation efficiencies for Wi-Fi 7 MIMO system: (a) 2.4 GHz band, and (b) 5 GHz and 6 GHz bands.

band, the current has high intensity across the whole geometry, especially around the ladder, U-shape slots, and shorting plate. However, going up in frequencies, the current intensity moves towards the feeding plate and the edge of the U-slot as it forms a folded $\lambda/4$ monopole.

The antenna radiation efficiency for both simulated model and fabricated prototype measured on 120 mm ground plane is shown in Fig. 6. The average efficiency for 2.4 GHz band is found to be around 70% while for 5 GHz and 6 GHz band, the antenna efficiency is around 80% which shows good radiation performance for the design.

The peak gain of the antenna is measured and plotted across the frequency bands in Fig. 7. The peak is measured by calculating the average gain across the azimuth angles (0–360 degrees) then finding the maximum value across elevation angles. It is important for a Wi-Fi 7 antenna to have a good gain across the three bands to meet the Effective Isotropic radiated Power (EIRP) requirements and provide good coverage area around the element; however, having high peak gain results in more directive behavior and could affect the omnidirectional pattern of the design. Fig. 7 shows peak gains around 1.5–2 dBi at 2.4 GHz band and 3–5 dBi at 5 GHz and 6 GHz which presents a good antenna gain performance for this design. The horizontal and vertical cuts of the radiation pattern of the design are shown in the next section where combined MIMO performance is also presented.

3. ANALYSIS OF MIMO ANTENNA SYSTEM

In this section, two identical antennas of the proposed design in the previous section are implemented on the same plane with an 80 mm spatial distance on 120 mm diameter ground plane that has two slots on its plane to improve isolation between elements without increasing spatial distance between them. Each antenna is mirrored across about the z-axis as shown in Fig. 8 where the simulation model and the fabricated prototype for the proposed MIMO system are shown. Each slot on the ground plane has a length of GL = 80 mm and a width of Gw = 5 mm optimized to improve isolation specially at 2.4 GHz band without affecting radiating performance of the elements.

The passive isolation measured in dB between the two elements is shown in Fig. 9. Measured and simulated isolations are in acceptable agreement across Wi-Fi 7 frequency bands with minor variations caused by antenna positioning on ground plane and slight attenuation from RF connections at various frequencies. It can be noticed from Fig. 9 that the worst passive isolation between the two antenna ports has a value of 31 dB for Wi-Fi 7 bands which expresses an excellent performance and very low mutual coupling. This is crucial for Wi-Fi 7 applications since high modulation rate (4K QAM) has very crowded and extremely close symbols in its constellation map, so any small loss of energy could lead to reading a wrong symbol. In Fig. 10, the effect of ground plane slots is presented and compared with no-slots ground plane. It can be noticed that introducing ground slots helps improve isolation by up to 6 dB especially at the 2.4 GHz band without increasing the spatial distance between MIMO antennas. This is reasoned due to common ground plane between antennas. With presenting slots, the ground current of each antenna is forced to travel longer distances, and hence ground currents at Wi-Fi bands are coupled less between each other. The slots shape was chosen like this to introduce higher impedance for ground currents of each antenna to reduce its effect on the other antenna. The size and location of the slots are crucial to tuning the isolation at the required frequency (In this case 2.45 GHz) and were optimized using multiple trials to improve isolation without reducing antenna performance.

Individual and combined radiation patterns of horizontal cuts at theta 60 degrees are shown for frequencies of 2.45 GHz, 5.5 GHz, and 6.5 GHz in Figs. 11(a), (b), and (c). In order to measure the patterns, one antenna is terminated by 50 ohms while the other is being measured. The two patterns are then combined to create a composite omnidirectional pattern that surrounds the entire system. To achieve omnidirectional pattern in the three bands, the orientation and placement of each PIFA in relation to the other is crucial. Additionally, at frequencies 2.45 GHz, 5.5 GHz, and 6.5 GHz, respectively, the aver-

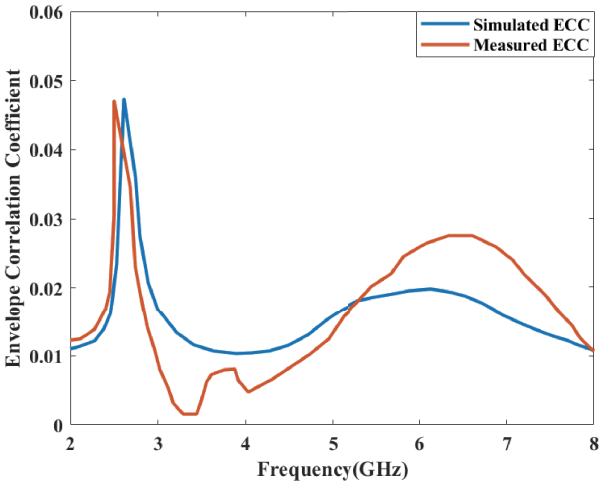

FIGURE 14. Simulated and measured ECC for the Wi-Fi 7 MIMO system.

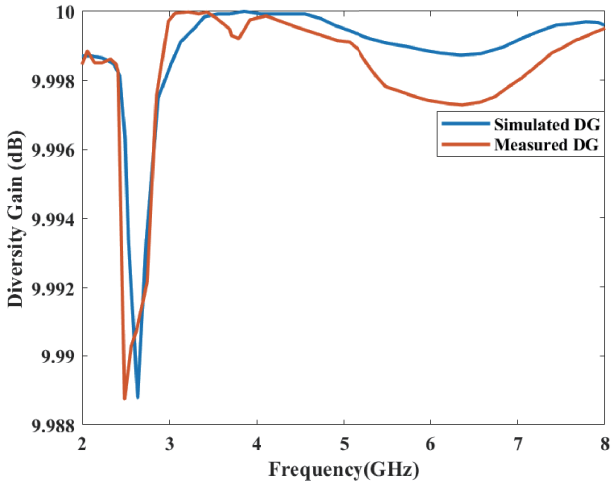

FIGURE 15. Simulated and measured DG for the Wi-Fi 7 MIMO system.

age realized gain observed from the measured combined radiation patterns on ground plane is found to be 2.1 dBi, 3.9 dBi, and 3.7 dBi. In Fig. 12, vertical cuts across elevation angles of ground plane measurements are plotted for frequencies 2.45 GHz, 5.5 GHz, and 6.5 GHz, respectively. The finite ground plane effect shifts the peak gain to higher elevation angles instead of the horizon. It can be found that the composite peak gain is around 2.3 dBi, 4.1 dBi, and 5.2 dBi at 2.45 GHz, 5.5 GHz, and 6.5 GHz, respectively.

Figures 13(a) and (b) show the measured port radiation efficiencies for the two elements on the ground plane for the Wi-Fi 7 bands. By dividing the realized measured gain from the chamber by the directivity across the entire sphere, the radiation efficiency of each port is calculated. The 2.4 GHz ground plane measurement has an average efficiency of roughly 68% for both antennas, while the 5 GHz and 6 GHz measurements have an average port efficiency of roughly 82%, which demonstrates the Wi-Fi 7 MIMO system's good radiation performance.

The correlation between the antenna elements is measured using a crucial parameter called ECC. In order to achieve the necessary Wi-Fi 7 MIMO performance, a low value of ECC (preferably less than 0.1 across all three bands) indicates an excellent isolation (low correlation) between the antennas, which leads to independent (Tx/Rx) RF channels in the MIMO system [20].

Figures 14 and 15 show the simulated and measured ECC and DG values of the Wi-Fi 7 MIMO system. Using the below formula utilizing far field electric field components, the ECC has been determined [20, 21]:

$$\rho_{e,ij} = \left| \frac{\int_0^{2\pi}\int_0^{\pi}\left(XPR\cdot E_{\theta i}\cdot E^*_{\theta j}\cdot P_\theta + XPR\cdot E_{\phi i}\cdot E^*_{\phi j}\cdot P_\phi\right)\sin(\theta)d\theta d\phi}{\sqrt{\prod_{k=i,j}\int_0^{2\pi}\int_0^{\pi}\left(XPR\cdot E_{\theta k}\cdot E^*_{\theta k}\cdot P_\theta + XPR\cdot E_{\varphi k}\cdot E^*_{\varphi k}\cdot P_\phi\right)\sin(\theta)d\theta d\phi}} \right|^2 \tag{2}$$

where Ei and Ej are the first and second elements' (i and j) respective electric field complex components across theta angles (θ). The electric field components Ei and Ej are also present, in the phi angles (φ). The cross-polarization ratio, or XPR, accounts for the difference between the received wave's vertical and horizontal polarizations. The theta and phi power densities are represented by $P\theta$ and $P\varphi$, respectively. Uniform power densities can be considered throughout elevation and azimuth angles, and XPR might be set to 1 to assume no polarization variations across the antennas, simplifying the calculations for Equation (2).

When the antennas in a MIMO system receive an RF signal, the DG, which is known as the quantitative improvement in signal-to-noise ratio, is computed using the formula [22]:

$$DG = 10 * \sqrt{(1-\rho_{e,ij})} \tag{3}$$

The amplitude and phase of the electric field components in the theta and phi planes were computed from the ground plane measurements and used in a MATLAB script to handle the electric field data and process the ECC and DG as in Equations (2) and (3). From Figs. 14 and 15, it can be shown that the worst measured ECC is about 0.05, which equates a DG of 9.98 dB, demonstrating the antennas' strong decoupling throughout the Wi-Fi 7 bands, a necessary condition for MIMO performance.

Table 3 compares the proposed design from this work with previously published research. The suggested design has good

TABLE 3. Comparison of the presented antenna system and existing literature.

	Type	**Frequency Bandwidth**	**Dimensions ($L \times W \times H$) (mm^3)**	**Performance**
Proposed Design	Loaded PIFA antenna	2400–2495 MHz 5150–5895 MHz 5945–7125 MHz	$14.5 \times 17 \times 3$	8 dB return loss. Peak gain 1.5–2 dBi at 2.4 GHz 3–5 dBi at 5 GHz and 6 GHz Avg. radiation efficiency 70% for 2.4 GHz and 80% for 5 GHz/6 GHz. MIMO isolation $>$ 30 dB.
12	Loaded slot antenna	2400–2495 MHz 5150–5895 MHz 5945–7125 MHz	$27 \times 0.8 \times 20$	Better than 6 dB return loss. gain -7 dBi at 2.4 GHz 4–7 dBi at 5 GHz and 6 GHz. radiation efficiency 17–20% for 2.4 GHz and 66–80% for 5 GHz/6 GHz. No MIMO proposed.
13	Printed L-antenna	2400–2495 MHz 5150–5895 MHz 5945–7125 MHz	$43 \times 0.4 \times 3$	Better than 10 dB return loss. gain 1–2 dBi at 2.4 GHz 1-3 dBi at 5 GHz and 6 GHz. radiation efficiency 80% for 2.4 GHz and 60–80% for 5 GHz/6 GHz. No MIMO proposed.
14	Printed Inverted F-antenna	2400–2495 MHz 5150–5895 MHz 5945–7125 MHz	$14.5 \times 0.8 \times 4$	Better than 10 dB return loss. gain 2–3 dBi at 2.4 GHz 4.2–6 dBi at 5 GHz and 6 GHz. radiation efficiency 45% for 2.4 GHz and 65% for 5 GHz/6 GHz. MIMO isolation $>$ 15 dB.
15	Printed Inverted U-shape antenna	2400–2495 MHz 5150-5895 MHz 5945-7125 MHz	$30 \times 0.5 \times 6$	Better than 7.4 dB return loss. gain 3–4 dBi at 2.4 GHz 4.7–6 dBi at 5 GHz and 6 GHz. radiation efficiency 70% for 2.4 GHz and 77–86% for 5 GHz/6 GHz. MIMO isolation $>$ 13 dB.
16	printed planar mirror-F antenna	2400–2495 MHz 5150–5895 MHz 5945–7125 MHz	$48 \times 1 \times 8$	Better than 8 dB return loss. gain 4 dBi at 2.4 GHz 4.54 dBi at 5 GHz and 6 GHz. radiation efficiency Not reported. MIMO isolation $>$ 15 dB.
17	Printed L-antenna with shorting stripes	2400–2495 MHz 5150–5895 MHz 5945–7125 MHz	$19.4 \times 0.8 \times 6.2$	Better than 10 dB return loss. No gain value reported. radiation efficiency 50–70% for 2.4 GHz and 40–80% for 5 GHz/6 GHz. MIMO isolation $>$ 12.5 dB.
18	Printed monopole-PIFA	2400–2495 MHz 5150–5895 MHz 5945–7125 MHz	$56 \times 0.8 \times 21.06$	Better than 10 dB return loss. gain 2–3 dBi at 2.4 GHz 4–5 dBi at 5 GHz and 6 GHz. radiation efficiency not reported. No MIMO isolation reported.

performance in terms of matched return loss across Wi-Fi 7 bands, MIMO passive isolation between elements, realized gain, omnidirectional patterns, port efficiencies, ECC, and DG over a wide frequency range.

4. CONCLUSION

A loaded low-profile 2 × 2 MIMO antenna system for Wi-Fi 7 applications has been analyzed in this work to be used in small low-profile application such as automotive field in front side mirrors or front dashboard, and consumer products in laptops and internet wireless routers. The presented design is based on a loaded PIFA on FR4 material with slots on its horizontal plane that operates on the Wi-Fi 7 three bands (2.4 GHz, 5 GHz, and 6 GHz). The MIMO system elements are separated by 80 mm spatial distances with slots on the ground plane that help achieve 30 dB passive isolation without increasing the distance which is a necessary requirement for Wi-Fi 7 performance specially at high modulation rates (4K QAM). Simulation model was built using HFSS software, and then a fabricated prototype was measured on 120 mm ground plane in an anechoic chamber. The performance of the design shows return loss performance better than 8 dB, peak gain 1.5–2 dBi at 2.4 GHz and 3–5 dBi at 5 GHz and 6 GHz, and radiation efficiency 70% for 2.4 GHz and 80% for 5 GHz/6 GHz. A 2 × 2 MIMO system was analyzed and presented using two identical elements of the proposed design but with different orientations. Across the active three Wi-Fi 7 bands, the MIMO system exhibits passive isolation better than 30 dB, ECC less than 0.05, and DG greater than 9.98 dB. In general, due to their reasonable size and good RF performance, the presented antenna design and MIMO system perform well enough to be used for low-profile Wi-Fi 7 applications.

ACKNOWLEDGEMENT

The authors would like to acknowledge Oakland University for providing measurements facilities and simulation tools.

REFERENCES

[1] Ghouz, H. H., "Novel compact and dual-broadband microstrip MIMO antennas for wireless applications," *Progress In Electromagnetics Research B*, Vol. 63, 107–121, 2015.

[2] Yacoub, A. M., M. O. Khalifa, and D. N. Aloi, "Wide band raised printed monopole for automotive 5G wireless communications," *IEEE Open Journal of Antennas and Propagation*, Vol. 3, 502–510, 2022.

[3] Yacoub, A., M. Khalifa, and D. N. Aloi, "Wide bandwidth low profile PIFA antenna for vehicular sub-6 GHz 5G and v2x wireless systems," *Progress In Electromagnetics Research C*, Vol. 109, 257–273, 2021.

[4] Yacoub, A., M. Khalifa, and D. N. Aloi, "Compact 2 x 2 automotive MIMO antenna systems for sub-6 GHz 5G and v2x communications," *Progress In Electromagnetics Research B*, Vol. 93, 23–46, 2021.

[5] Sim, C.-Y.-D., J. Kulkarni, S.-H. Wang, S.-Y. Zheng, Z.-H. Lin, and S.-C. Chen, "Low-profile laptop antenna design for Wi-Fi 6E band," *IEEE Antennas and Wireless Propagation Letters*, Vol. 22, No. 1, 79–83, Jan. 2023.

[6] FCC, "Report and order and further notice of proposed rulemaking; In the matter of unlicensed use of the 6 GHz band (ET Docket No. 18–295); Expanding flexible use in mid-band spectrum between 3.7 and 24 GHz (GN Docket No. 17–183)," Apr. 2020.

[7] Korolev, N., I. Levitsky, and E. Khorov, "Analytical model of multi-link operation in saturated heterogeneous Wi-Fi 7 networks," *IEEE Wireless Communications Letters*, Vol. 11, No. 12, 2546–2549, Dec. 2022.

[8] Khorov, E., I. Levitsky, and I. F. Akyildiz, "Current status and directions of IEEE 802.11be, the future Wi-Fi 7," *IEEE Access*, Vol. 8, 88 664–88 688, 2020.

[9] Yacoub, A. and D. N. Aloi, "Low-profile automotive antenna systems for MIMO 5G and L1/L5 GNSS communications," in *2022 16th European Conference on Antennas and Propagation (EUCAP)*, Madrid, Spain, Mar. 2022.

[10] Deng, C., X. Fang, X. Han, X. Wang, L. Yan, R. He, Y. Long, and Y. Guo, "IEEE 802.11be Wi-Fi 7: New challenges and opportunities," *IEEE Communications Surveys and Tutorials*, Vol. 22, No. 4, 2136–2166, 2020.

[11] See, C. H., R. A. Abd-Alhameed, Z. Z. Abidin, N. J. McEwan, and P. S. Excell, "Wideband printed MIMO/diversity monopole antenna for WiFi/WIMAX applications," *IEEE Transactions on Antennas and Propagation*, Vol. 60, No. 4, 2028–2035, Apr. 2012.

[12] Han, T.-Y., W.-T. Hsieh, K.-H. Jheng, S.-H. Wang, and C.-Y.-D. Sim, "Design of laptop antenna for WLAN and Wi-Fi 6E applications," in *2021 International Symposium on Antennas and Propagation (ISAP)*, Taipei, Taiwan, Oct. 2021.

[13] Jhang, W.-C. and J.-S. Sun, "Small antenna design of triple band for WiFi 6E and WLAN applications in the narrow border laptop computer," *International Journal of Antennas and Propagation*, Vol. 2021, Jul. 2021.

[14] Lee, C.-T., C.-C. Wan, and S.-W. Su, "Multi-laptop-antenna designs for 2.4/5/6 GHz WLAN and 5G NR77/78/79 operation," in *2020 International Symposium on Antennas and Propagation (ISAP)*, 421–422, Electr Network, Jan. 25-28, Jan. 2021.

[15] Su, S.-W. and C.-C. Wan, "Asymmetrical, self-isolated laptop antenna in the 2.4/5/6 GHz Wi-Fi 6E bands," in *2021 International Symposium on Antennas and Propagation (ISAP)*, Taipei, Taiwan, Oct. 2021.

[16] Li, A., B. Feng, and X. Ding, "A wideband omnidirectional MIMO antenna for WiFi-6E applications," in *2022 IEEE 5th International Conference on Electronic Information and Communication Technology (ICEICT)*, 834–836, 2022.

[17] Cai, C.-A., K.-Y. Kai, and W.-J. Liao, "A WLAN/WiFi-6E MIMO antenna design for handset devices," in *2021 International Symposium on Antennas and Propagation (ISAP)*, Taipei, Taiwan, Oct. 2021.

[18] Chang, C.-C., Y.-F. Lin, M.-T. Nguyen, Y.-X. Liu, H.-T. Chen, and H.-M. Chen, "Design of MIMO antennas for WiFi/5G small cell applications," in *2021 International Symposium on Antennas and Propagation (ISAP)*, Taipei, Taiwan, Oct. 2021.

[19] Chattha, H. T., Y. Huang, X. Zhu, and Y. Lu, "An empirical equation for predicting the resonant frequency of planar inverted-F antennas," *IEEE Antennas and Wireless Propagation Letters*, Vol. 8, 856–860, 2009.

[20] Sharawi, M. S., A. T. Hassan, and M. U. Khan, "Correlation coefficient calculations for MIMO antenna systems: A comparative study," *International Journal of Microwave and Wireless Technologies*, Vol. 9, No. 10, 1991–2004, Dec. 2017.

[21] Elshirkasi, A. M., A. A. Al-Hadi, M. F. Mansor, R. Khan, and P. J. Soh, "Envelope correlation coefficient of a two-port MIMO

terminal antenna under uniform and gaussian angular power spectrum with user's hand effect," *Progress In Electromagnetics Research C*, Vol. 92, 123–136, 2019.

[22] Beegum, S. F. and S. K. Mishra, "Compact WLAN band-notched printed ultrawideband MIMO antenna with polarization diversity," *Progress In Electromagnetics Research C*, Vol. 61, 149–159, 2016.

[23] Yacoub, A. and D. Aloi, "Low-profile MIMO antenna system for vehicular Wi-Fi 7 wireless communications," in *2023 Xxxvth General Assembly and Scientific Symposium of The International Union of Radio Science (URSI GASS)*, 1–4, 2023.